IOP Publishing J. Phys. Energy 3 (2021) 032003 https://doi.org/10.1088/2515-7655/abebca

Journal of Physics: Energy

OPEN ACCESS

RECEIVED
22 October 2020

REVISED
27 January 2021

ACCEPTED FOR PUBLICATION
3 March 2021

PUBLISHED
16 April 2021

TOPICAL REVIEW

Emerging inorganic solar cell efficiency tables (version 2)

Andriy Zakutayev[1], Jonathan D Major[2], Xiaojing Hao[3], Aron Walsh[4,5], Jiang Tang[6], Teodor K Todorov[7], Lydia H Wong[8] and Edgardo Saucedo[9,*]

[1] National Renewable Energy Laboratory (NREL), Golden, CO 80401, United States of America
[2] Stephenson Institute for Renewable Energy, Department of Physics, University of Liverpool (UL), Liverpool L69 7ZF, United Kingdom
[3] Australian Centre for Advanced Photovoltaics, School of Photovoltaic and Renewable Energy Engineering, University of New South Wales (UNSW), Sydney, NSW 2052, Australia
[4] Department of Materials, Imperial College London (ICL), Exhibition Road, London SW7 2AZ, United Kingdom
[5] Yonsei University (YU), Seoul 03722, Republic of Korea
[6] Wuhan National Laboratory for Optoelectronics, Huazhong University of Science and Technology (HUST), 430074 Wuhan, People's Republic of China
[7] IBM Thomas J. Watson Research Center, Yorktown Heights, New York 10598, United States of America
[8] School of Materials Science & Engineering, Nanyang Technological University (NTU), Singapore 639789, Singapore
[9] Universitat Politècnica de Catalunya (UPC), Campus Diagonal-Besòs, 08930 Sant Adrià del Besòs- Barcelona, Spain
[*] Author to whom any correspondence should be addressed.

E-mail: edgardo.saucedo@upc.edu

Keywords: thin film inorganic photovoltaics, emerging photovoltaic technologies, conversion efficiency, solar energy

Abstract

This paper presents the second version of the efficiency tables of materials considered as emerging inorganic absorbers for photovoltaic solar cell technologies. The materials collected in these tables are selected based on their progress in recent years, and their demonstrated potential as future photovoltaic absorbers. The first part of the paper consists of the guidelines for the inclusion of the different technologies in this paper, the verification means used by the authors, and recommendation for measurement best practices. The second part details the highest world-class certified solar cell efficiencies, and the highest non-certified cases (some independently confirmed). The third part highlights the new entries including the record efficiencies, as well as new materials included in this version of the tables. The final part is dedicated to review a specific aspect of materials research that the authors consider of high relevance for the scientific community. In this version of the efficiency tables, we are including an overview of the latest progress in quasi one-dimensional absorbers, such as antimony chalcogenides, for photovoltaic applications.

Abbreviations

Eff. (%)	conversion efficiency obtained under AM1.5 illumination in percentage
V_{OC} (V)	open circuit voltage in volts
J_{SC} (mA cm^{-2})	short circuit current in milli-Amperes by square centimetre
FF (%)	fill factor in percentage
E_g (eV)	bandgap in electronvolt
AZO	ZnO:Al
ITO	In_2O_3:SnO_2
Spiro-OMeTAD	2,2′,7,7′-tetrakis[N,N-di(4-methoxyphenyl)amino]-9,9′-spirobifluorene ($C_{81}H_{68}N_4O_8$)
TBAI	tetrabutylammonium iodide
EDT	1,2-ethanedithiol
PTB7	poly[[4,8-bis[(2-ethylhexyl)oxy]benzo[1,2-b:4,5-b']dithiophene-2,6-diyl][3-fluoro-2-[(2-ethylhexyl)carbonyl]thieno[3,4-b]thiophenediyl]] (($C_{41}H_{53}FO_4S_4$)$_n$)
ARC	anti-reflection coating
$CuPc^+$	copper phthalocyanine

PTAA	poly[bis(4-phenyl)(2,4,6-trimethylphenyl)amine ($(C_{21}H_{19}N)_n$)
PCBM	[6,6]-phenyl C61 butyric acid methyl ester ($C_{72}H_{14}O_2$)
mp-TiO_2	mesoporous TiO_2
TiO_2-BL	TiO_2 blocking layer
PCPDTBT	poly[N-9′-heptadecanyl-2,7-carbazole-alt-5,5-(4,7-di-2-thienyl-2′,1′,3′-benzothiadiazole] ($(C_{43}H_{47}N_3S_3)_nC_{12}H_{10}$)
PEDOT:PSS	poly(2,3-dihydrothieno-1,4-dioxin)-poly(styrenesulfonate)
P3HT	poly(3-hexylthiophene-2,5-diyl) ($(C_{10}H_{14}S)_n$)
PEG	poly(ethylene glycol)
F8	poly(9,9-di-noctylfluorenyl-2,7-diyl)
Q-1D	quasi one-dimensional

1. Introduction

1.1. Scope of the paper

Several photovoltaic technologies have now reached the point where they are mature enough, to reach the market and the progress in their power conversion efficiencies are summarized regularly in 'Solar Cell Efficiency Tables' [1]. Crystalline and multi-crystalline Si modules are the industrial standard but a-Si, Cu(In, Ga)(S, Se)$_2$, CdTe, organic photovoltaic, dye-sensitized solar cells, etc have all been commercialized to varying degrees of success. Whilst these technologies could feasibly cover the majority of photovoltaic applications, increasing the diversity of viable photovoltaic materials will allow for greater adaptability as the technology continues to expand and develop. Additionally, most of the established platforms face challenges related to either the use of critical raw materials, toxic elements, long-term stability, conversion efficiency limitations, cost or low technological flexibility (e.g. incompatibility with flexible substrates, or transparent concepts). These are all important considerations that must be taken into account as the field begins to look towards an era of terawatt level photovoltaic power generation.

The limitations of the mature technologies encourage a continued search for new materials, as none of the established technologies represent the 'perfect' photovoltaic material. The purpose of continued exploratory research is to identify absorbers that can bring additional benefits and/or may allow the development of novel applications. New inorganic materials including chalcogenides (sulphides, selenides, tellurides), oxides, pnictides (nitrides, phosphides), halides (mainly bromides and iodides) and mixed-anion compounds (e.g. sulfo-iodites) have proved a fruitful area of research and attracted a lot of attention. There are numerous examples published in recent years showcasing the capability of these materials to act as photovoltaic absorbers. Respectable device efficiencies have been reported for numerous cell platforms despite their typically being only limited attempts at fabrication and often with only specific groups contributing to their progresses. Several of these emerging cell structures have shown enough development to identify them as potential future technological solutions. As a result, there has been a resurgent interest from the scientific community in emerging photovoltaic solar cell absorbers, as is shown in figure 1, where the number of papers published on this topic has increased significantly in the past decade. Notably, starting from around 300 papers published in this topic in 2011, almost 2000 were published in 2020 in total in the 4 main emerging inorganic photovoltaic technologies, implying an impressive annual growth rate close to 25% in the last 10 years. Even faster increase in number of publications has been happening in organic and hybrid materials, as discussed in the recent publication on 'Device Performance of Emerging Photovoltaic Materials (Version 1) [2].

Given the continually developing nature of the research field and the large number of emerging inorganic photovoltaic materials, this paper was conceived to collate information on the current status of the most promising materials in form of efficiency tables, collecting and summarizing the most relevant information available in the literature. This includes certified efficiencies in one of the six special centres available in the world, as well as independently measured examples with a description of the means of efficiency verification (or lack thereof). The main aim of these tables is to provide researchers working on emerging inorganic technologies with a valuable information resource by condensing all the spread information about these fascinating materials, but also to establish a forum for the discussion moving forward. It is hoped that these tables will evolve with the field and with input from the researchers in the community, informing future versions to include new champion devices or emerging technologies of note. This second edition of the tables [3] aims to support and inspire future research in the emerging inorganic solar cells.

1.2. Structure of the paper

The paper is structured in four sections, with the following details:

Section 1 is the present section, giving an overview of the paper, a description of its structure, an explanation about the criterion used to select the materials included in the different efficiency tables, and a

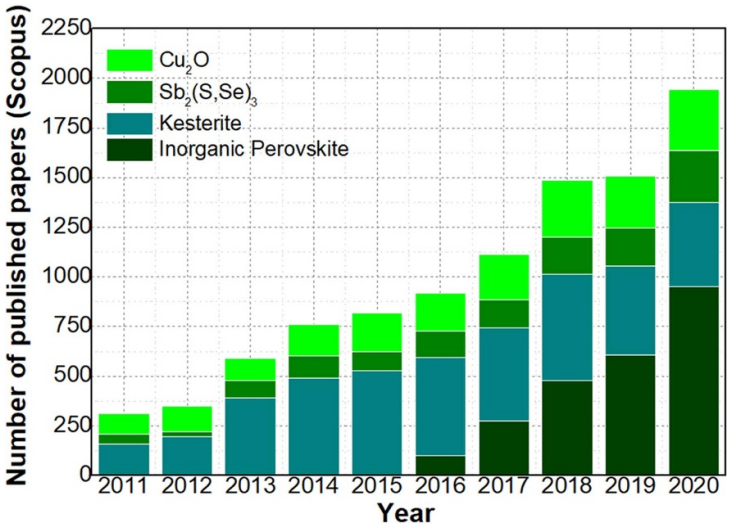

Figure 1. Number of published papers in the last 10 years referring to emerging photovoltaics, including kesterite, inorganic perovskite ($CsPbI_3$, $CsPbB_3$ and related materials), $Sb_2(S,Se)_3$ and Cu_2O (extracted from Scopus in January 2021).

description of the recommended procedures for the correct *J–V* in-house illuminated curve measurement, extraction of corresponding optoelectronic parameters, as well other additional devices information that the authors consider of high relevance for emerging photovoltaic technologies.

Section 2 contains the efficiency tables split into two categories. The first table summarizes all the world-class certifications available in the literature, and compiled by the authors. For this table we consider certified devices with efficiency higher than 5% and area larger than 0.1 cm^2. Exceptions of these considerations are summarized at the end of the table. The second table collects all the devices that are non-certified but can be confirmed using specific procedure, with efficiency higher than 1% and area larger than 0.1 cm^2. Exceptions of these considerations are also summarized at the end of the table. In each of these two tables, the materials are organized firstly depending on the type of compounds (oxides, chalcogenides, pnictides, halides, etc), and then in terms of complexity from less to more atoms in the structure.

Section 3 provides a brief description of new entries in terms of new efficiency records but also new materials included in the tables, with a brief review of the last and most impacting progresses reported in these technologies.

Section 4 aims to bring to the scientific community a perspective review of a specific topic that the authors have identified as very timely and with high relevance. In this second edition of the efficiency tables, the authors have invited Professor Jiang Tang from Huazhong University of Science and Technology (HUST), China, to review the last progresses in Q-1D materials for photovoltaic applications, including the impressive achievements in $Sb_2(S,Se)_3$ compounds.

1.3. Criterion for technology selection

For selecting the materials included in the efficiency tables, the authors have defined the following criterion:

Table 1 (World class certification): fully inorganic technologies with certified materials in one of the six world class certifying centres, with efficiency higher than 5% and area larger than 0.1 cm^2. Exceptions to these rules are collected separately at the end of the table.

Table 2 (Non world class certification or in house measurements): fully inorganic technologies of non-certified materials with efficiency higher than 1%, verification through external quantum efficiency (EQE) measurement, or independent confirmation by a second organization, and area larger than 0.1 cm^2. Exceptions to these rules are collected separately at the end of the table.

1.4. General guidelines for efficiency measurement

There are several important documents and organization that define solar cell efficiency measurements, including IEC 60904-3:2008 by International Electrotechnical Commission for general standards and ASTM G-173-03 by ASTM International for Test Methods and Reference Cells. Certification measurements following these standards are usually performed by one of the internationally recognized institutions, such as NREL (USA), AIST (Japan), CSIRO (Australia), Fraunhofer ISE (Germany), CNIM and NPVM (China) or a few commercial organizations (e.g. Newport), and the records certified by five of them (i.e. NREL, AIST, CSIRO, Fraunhofer ISE, and Newport) are published bi-annually in 'solar cell efficiency tables' [1] for

Table 1. List of certified single-junction record cells under global AM1.5 spectrum (1000 W m^{-2}) at 25 °C, including relevant optoelectronic parameters and important additional data (IEC 60 904-3: 2008, ASTM G-173-03 global).

Material	Eff. (%)	V_{OC} (V)	J_{SC} (mA cm^{-2})	FF (%)	Area (cm^2)	E_g (eV)	Device structure	Certifying centre/date	Comments
Sb_2Se_3 (substrate)	9.2	0.400	32.6	70.3	0.26	1.18	Glass/Mo/$MoSe_2$/Sb_2Se_3/ ZnO/AZO	CNIM (2018)	*Hebei Key Laboratory of Optic-Electronic Information Materials, Hebiei University, China* [4]. Substrate geometry structure incorporating core–shell nanowire approach. Absorber deposited by CSS.
Cu_2ZnSnS_4 (CZTS)	11.0 ± 0.2	0.731	21.74	69.3	0.2339	1.5	Glass/Mo/CZTS/CdS/ i-ZnO/ITO/Al/MgF_2	NREL (2017)	*UNSW* [5]. Absorber prepared by sputtering Cu/ZnS/SnS, and reactive annealing
$Cu_2ZnSn(S_{0.25}Se_{0.75})_4$ (CZTSSe)	12.6 ± 0.3	0.513	35.2	69.8	0.4209	1.13	Glass/Mo/CZTSSe/CdS/ ZnO/ITO/Ni/Al/MgF_2	Newport (2013)	*IBM* [6]. Absorber prepared by spin-coating a hydrazine-based solution, solution and reactive annealing.
$Cu_2ZnSn(S_ySe_{1-y})_4$ (CZTSSe)	12.62 ± 0.29	0.541	35.35	65.9	0.4804	NA	Glass/Mo/CZTSSe/CdS/ ZnO/ITO/Ni/Al/MgF_2	Newport (2018)	*DGIST* [7]. Absorber prepared by sputtering Sn/Cu/Zn and reactive annealing.
$Cu_2ZnSnSe_4$ (CZTSe)	12.50	0.491	37.37	68.2	0.24	1.04	Glass/Mo/CZTSe/CdS/ ZnO/AZO/Ni/Al/MgF_2	NPVM (2019)	*UNSW/Jinan University* [8]. Absorber prepared by sputtering Cu/Zn/Sn and reactive annealing in mixed Se/Ar vapor.
Notable exceptions									
Cu_2O	3.97[a]	1.204	7.37	44.70	0.15	2.2	MgF_2/Al/Al:ZnO/Ga_2O_3/ Cu_2O/Au	NREL (2014)	*MIT, Harvard University Cambridge and NREL* [9]. Electrochemical deposition.
$CsPbI_3$	13.58	1.1626	15.246	76.63	0.058	NA	Al/MoO_x/Spiro-OMeTAD/ $CsPbI_3$/TiO_2/SnO_2:F/ Glass/MgF_2	NREL (2017)	*NREL, University of Washington and University of Colorado* [10]. Coupled quantum dots films.
SnS	4.36[a]	0.372	20.2	58.0	0.24	1.1	Glass/Mo/SnS/SnO_2/ Zn(O,S):N/ZnO/ITO	NREL (2014)	*Department of Chemistry and Biology, Harvard University, Cambridge, USA* [11]. ALD deposition of absorber followed by annealing in H_2S.
Q-1D Sb_2Se_3 (superstrate)	7.6	0.420	29.9	60.4	0.091[b]	1.18	Glass/ITO/CdS/Sb_2Se_3/Au	CNIM (2017)	*Sargent Joint Research Center, Wuhan National Laboratory for Optoelectronics and School of Optical and Electronic Information, Huazhong University of Science and Technology, Wuhan, China* [12]. Vapour transport deposition.

(Continued)

Table 1. (Continued.)

Material	Eff. (%)	V_{OC} (V)	J_{SC} (mA cm^{-2})	FF (%)	Area (cm^2)	E_g (eV)	Device structure	Certifying centre/date	Comments
Q-1D $Sb_2(S,Se)_3$	10.0	0.655	24.07	63.5	0.0889	1.49	Glass/FTO/CdS/Sb_2Se_3/Spiro-OMeTAD/Au	CNIM (2019)	*University of Science and Technology of China, China* [13]. *Hydrothermal deposition and annealing.*
PbS	9.88	0.635	21.6	71.9	0.05[b]	NA	Glass/ITO/ZnO/PbS(TBAI)/PbS(EDT)/Au	Newport (2015)	*Wuhan National Laboratory for Optoelectronics and School of Optical and Electronic Information, Huazhong University of Science and Technology, Wuhan, China* [14]. Spin coating of PbS colloidal quantum dots.
$AgBiS_2$	6.31	0.450	22.1	63.0	0.017[b]	1.3	Glass/ITO/ZnO/$AgBiS_2$/PTB7/MoO_3	Newport (2016)	*ICFO—Institut de Ciències Fotòniques, The Barcelona Institute of Science and Technology, Barcelona, Spain* [15]. Layer-by-layer spin coat deposition from nanocrystal solution.

[a] Certified efficiency below 5%.

[b] Area of the certified cell below 0.1 cm^2 (total area).

NA—not available.

Table 2. List of non-certified single-junction record cells under global AM1.5 spectrum (1000 W m^{-2}) at 25 °C, including relevant optoelectronic parameters, the means of verification and important additional data (IEC 60 904-3: 2008, ASTM G-173-03 global).

Material	Eff. (%)	V_{OC} (V)	J_{SC} (mA cm^{-2})	FF (%)	Area (cm^2)	E_g (eV)	Device structure	Means of verification	Institutions and Comments
Pnictides									
Zn_3P_2	6.0	0.492	14.9	71.0	0.70	NA	ZnS/Mg/Ag:Zn_3P_2/Ag	No EQE results	*U. Delaware* [16]. CVT grown thick wafer absorber measured in AMI illumination. Measured under a simulated intensity of 87.5 mW cm^{-2}.
$ZnSnP_2$	3.44	0.47	12.3	59	0.785	1.68	Al/ZnO:Al/ZnO/(Cd, Zn)S/$ZnSnP_2$/Cu	EQE, In-house	*Ritsumeikan University* [17]. Bulk ZnSnP2 crystals with 200 um thickness grown by flux method.
Oxides									
$BiMnO_3$:$BiMn_2O_5$	4.2	1.5	4.9	58	0.5	1.25	Nb:$SrTiO_3$/$BiMnO_3$:$BiMn_2O_5$/ In_2O_3:SnO_2	EQE, In-house	*INRS Canada* [18]. Absorbers grown by PLD on single crystal substrate.
Chalcogenides									
$CuSbSe_2$	4.7	0.336	26.3	53.0	0.2	NA	Glass/Mo/$CuSbSe_2$/ZnO/AZO	EQE, In-house	*National Renewable Energy Laboratory, Golden, USA* [19]. Sputtering from binary Cu_2Se and Sb_2Se_3 targets.
$CuSbS_2$	3.2	0.470	15.6	43.6	0.45	1.4–1.9	Glass/Mo/$CuSbS_2$/CdS/ ZnO/AZO	EQE, In-house	*New and Renewable Energy Research Division, Korea Institute of Energy Research, Daejeon, South Korea* [20]. Sulfurization of nanoparticle inks.
Cu_2CdSnS_4	7.96	0.624	22.3	57.2	0.16	1.42	Glass/Mo/CCdTS/CdS/ ITO/Ag	EQE, In-house	*NTU, Singapore* [21]. Absorber prepared by spin-coating using 2-methoxyethanol-based solution.
Cu_2BaSnS_4 (substrate)	1.7	0.698	5.3	46.9	0.2	2.01	Glass/Mo/CBaTS/CdS/ZnO/ ITO/Al	EQE, In-house	*Central South University, UNSW, Shen Zhen University, Xiamen University* [22]. Absorber prepared by spin-coating using a 2-methoxyethanol-based solution.
Cu_2BaSnS_4 (superstrate)	2.0	0.933	5.1	42.9	0.2	2.04	CdS:O/CdS/ZnO/AZO	EQE, In-house	*The University of Toledo* [23]. Absorber prepared by sputtering method.
Cu_2FeSnS_4	3.0	0.610	9.3	52.0	0.1	1.5	ITO/Cu-NiO/CFeTS/ Bi_2S_3/ZnO/Al	EQE, In-house	*Indian Association for the Cultivation of Science* [24]. Absorber prepared by SILAR method.

(Continued)

Table 2. (Continued.)

Material	Eff. (%)	V_{OC} (V)	J_{SC} (mA cm^{-2})	FF (%)	Area (cm^2)	E_g (eV)	Device structure	Means of verification	Institutions and Comments
$Cu_2CdSn(S_{0.xx}Se_{0.yy})_4$	2.8	0.356	18.8	41.6	0.405	1.55	Glass/Mo/CCdTSSe/CdS/ ZnO/ITO/Al	EQE, In-house	*Changchun Institute of Applied Chemistry, Chinese Academy of Sciences* [25]. Absorber prepared by spin-coating an ethanol, butyldithiocarbamic acid, and thioglycolic acid -based solution.
$Cu_2BaSn(S_{0.xx}Se_{0.yy})_4$	5.2	0.611	17.4	48.9	0.425	1.55	Glass/Mo/CBaTSSe/CdS/ ZnO/ITO/Ni/Al	EQE, In-house	*Duke University, IBM* [26]. Absorber prepared by co-sputtering using Cu, Sn, and BaS
$Cu_2ZnGe(S_{0.xx}Se_{0.yy})_4$	6.0	0.617	NA	NA	0.25	1.47	Glass/Mo/CZGeSSe/CdS/ ZnO/AZO/Ni/Al	EQE, In-house	*ZSW, CNRS* [27]. Absorber prepared by doctor-blade coating a DMF-based solution.
$Cu_2ZnGeSe_4$	8.5	0.625	24.4	55.7	0.52	1.39	Glass/Mo/CZGSe/CdS/ IZO/AZO/Ni/Al	EQE, in-house	Institut des Materiaux *Jean Rouxel (IMN)* [28]. HCl and $(NH_4)_2S$ solution for surface treatment, air annealing at 200 °C for 60 min.
$Ag_2ZnSnSe_4$	5.18	0.504	21.0	48.7	0.45	1.35	FTO/AgZTSe/MoO_3/ITO/ Ni/Al	EQE, In-house	*IBM, UCSD* [29]. Absorber prepared by coevaporation of Ag, Zn, Sn, and cracked Se.
$Cu_2ZnCdSnS_4$	12.60	0.640	27.8	71.0	0.16	1.34	Glass/Mo/CZCTS/CdS/ ITO/Ag	EQE, in-house, active area	*Shenzhen University* [30]. Device annealed at 300 °C in air for 8 min.
$(Ag_{0.05–0.3}Cu_{0.95–0.7})_2ZnSn(S,Se)_4$	11.2	0.464	36.2	66.5	0.21	Graded	Glass/Mo/ACZTSSe/CdS/ ZnO/ITO/Ag	EQE, in-house	*Henan University, China* [31]. Spin coating of ethanol based solutions.
$(Ag_{0.05}Cu_{0.95})_2(Zn_{0.75}Cd_{0.25})S_4$	10.1	0.650	23.4	66.2	0.16	1.4	Glass/Mo/ACCdZTS/CdS/ ITO/Ag	EQE, in-house	*NTU, Singapore; HZB, Germany* [32]. Spin coating of 2-methoxyethanol based solution.
$Cu_2Zn(Sn_{0.78}Ge_{0.22})Se_4$	12.3	0.527	32.2	72.7	0.519	1.11	Glass/Mo/CZTGTSe/CdS/ ZnO/AZO/Ag/ARC	EQE, in-house	*AIST, Japan* [33]. Co-evaporation and reactive annealing.
$(Li_{0.06}Cu_{0.94})_2ZnSn(S,Se)_4$	11.6	0.531	33.7	64.8	0.285	1.13	Glass/SiO_x/Mo/LiCZTSSe/ CdS/ZnO/AZO/Ni/Al/MgF_2	EQE, in-house	*EMPA, Switzerland; Universidad Autónoma de Madrid, Spain; HZB, Germany* [34]. Spin coating of DMSO based solution.
$Cu_2(Zn_{0.95}Mn_{0.05})Sn(S,Se)_4$	8.9	0.418	33.7	63.3	0.34	1.06	Glass/Mo/CMZTSSe/CdS/ ZnO/AZO/Ni/Al	EQE	*Nankai University, China; National Institute of Material Science, Japan* [35]. Spin coating of 2-methoxyethanol based solution.
$Cu_2Zn_{0.96}Mg_{0.04}Sn(S,Se)_4$	7.2	0.419	37.2	46.5	0.3	1.01	Glass/SiO_x/Mo/CZMTSSe/ CdS/i-ZnO/AZO/Ni/ Al/MgF2		*Universidad Autónoma de Madrid, Spain* [36]. Precursor solution prepared by dimethyl sulfoxide (DMSO).

(Continued)

Table 2. (Continued.)

Material	Eff. (%)	V_{OC} (V)	J_{SC} (mA cm^{-2})	FF (%)	Area (cm^2)	E_g (eV)	Device structure	Means of verification	Institutions and Comments
Cu_2SnS_3	5.1	0.290	34.5	51.3	0.3	0.95	Glass/Mo/CTS/CdS/ i-ZnO/AZO/Ni/Al	EQE, in-house	*Ritsumeikan University, Japan* [37]. Absorber prepared by Sputtering of Cu-SnS2 compound, and e-beam evaporation of NaF.
$Cu_2ZnSn_{0.91}I_{0.09}(S,Se)_4$	7.19	0.393	32.12	56.96	0.21	1.075	Mo-foil/CZTISSe/CdS/ i-ZnO/ITO/Ag	EQE, in house	*Fujian JIangxia University, Fuzhou, China* [38]. Absorber is deposited on flexible Mo foil by spin coating of precursor solution based on 1,2-ethanedithiol (edtH2) and 1,2-ethylenediamine (en) solution.
$Cu_2ZnSn_xGa_{1-x}(S,Se)_4$	10.8	0.455	36.48	65.05	0.21	1.162	Glass/Mo/CZTGSSe/CdS/ iZnO/ITO/Ag/MgF_2	EQE, in house	*Henan University* [31]. With ARC; thin film is deposited by spin coating of precursor solution based on ethylendiamine and 1,2 ethanedithiol.
$Cu_2Sn_{1-x}Ge_xS_3$	6.73	0.442	26.6	57.1	0.17	1.09	Glass/Mo/CTGS/CdS/ ZnO:Ga/Al	EQE, in-house	*Toyota Central Research & Development Laboratories, Japan* [39]. Co-sputtering Cu-Sn-Ge with two layer stack.
Notable exceptions									
Oxides									
Cu_2O	8.1	1.2	10.4	65.0	0.03[a]	2.2	MgF_2/Al:ZnO/$Zn_{0.38}Ge_{0.62}O$/ Cu_2O:Na/Au	No EQE results	*Kanazawa I. T* [40]. Cu_2O sheets oxidized from Cu foils
Bi_2FeCrO_6	8.1	0.84	20.6	46.0	NA[a]	1.4	Sn:In_2O_3/Bi_2FeCrO_6/$SrRuO_3$	EQE, In-house	*INRS Canada* [41]. PLD absorber with 3-layer stack.
Pnictides									
InP	7.3	0.57	17.4	73.0	0.0625[a]	1.32	Al/ZnO:Al/i-ZnO/ InP:Zn/Au-Zn-Au	EQE, In-house	*Purdue U., The U. of California, and The Pennsylvania State U* [42]. Pulsed laser deposition.
(In,Ga)N	3.0	1.8	2.6	64.0	0.046[a]	NA	SiO_2/Au/(Mg:GaN/GaN)/ (In,Ga)N/Si:GaN	No EQE results	*Texas Tech* [43]. MOCVD MQW absorber
$ZnSnN_2$	1.5	0.36	7.5	57.0	0.06[a]	1.4	Au/$ZnSnN_2$/Al_2O_3/SnO	No EQE results	*Ningbo, China* [44]. Sputtered absorber.
Halides									
BiI_3	1.2	0.607	5.3	37.6	0.04[a]	1.72	Au/F8/BiI_3/TiO_2/SnO_2:F[b]	EQE, In-house	*U. Bristol* [45]. Spin coating of $Bi(NO_3)_3$ and thiourea, followed by thermolysis at 200 °C to produce a homogeneous Bi_2S_3 film that is subsequently iodinated upon exposure to the I_2 gas.

(Continued)

Table 2. (Continued.)

Material	Eff. (%)	V_{OC} (V)	J_{SC} (mA cm^{-2})	FF (%)	Area (cm^2)	E_g (eV)	Device structure	Means of verification	Institutions and Comments
$CsPbBr_3$	10.91	1.498	9.78	74.47	0.09[a]	2.35	Ag/Spiro-OMeTAD/ $CsPbBr_3$/c-TiO2/ SnO_2:F[b]	EQE, In-house, reverse voltage	*Okinawa Institute of Science and Technology Graduate University (OIST), Japan and Hefei University of Technology, China* [46]. Thermal evaporation.
$CsPbI_3$	19.03	1.137	20.23	82.7	0.1	N.R.	Ag/Spiro-OMeTAD/ $CsPbI_3$/c-TiO_2/SnO_2:F[b]	EQE, In-house	*Shanghai Jiao Tong University, China* [47]. Spin coating and soft annealing.
$CsPbI_2Br$	16.79	1.32	15.32	83.29	0.09[a]	1.91	Au/Spiro-OMeTAD/ $CsPbI_2Br$/TiO_2/SnO_2:F[b]	EQE, In-house	*Shaanxi Normal University, China* [48]. Spin coating and soft annealing.
$CsPbIBr_2$	11.1	1.21	12.25	74.82	0.078	2.07	Ag/Spiro-OMeTAD/ PEG:$CsPbIBr_2$/TiO_2/SnO_2:F[b]	EQE, in-house	*Soochow University, China* [49]. Spin coating and soft annealing.
$CsPb_{0.75}Sn_{0.25}IBr_2$	11.53	1.21	12.57	75.8	0.1	1.78	Au/Spiro-OMeTAD/ $CsPb_{0.75}Sn_{0.25}IBr_2$/C60/ TiO_2/In_2O_3:SnO_2	EQE, In-house	*Tsinghua University-China, The University of Washington-USA, The Hong Kong University of Science and Technology-Hong Kong, City University of Hong Kong-Hong Kong* [50]. Spin coating and soft annealing.
$CsPb_{0.95}Eu_{0.05}I_2Br$	13.7	1.22	14.6	76.6	0.16	1.91	Au/Spiro-OMeTAD/ $CsPb_{0.95}Eu_{0.05}I_2Br$/$TiO_2$/ SnO_2:F[b]	EQE, In-house	*Wuhan U. Technology, EPFL, Nankai U* [51]. Precursor solution by spin coating. Some hysteresis is observed.
$CsSnBr_3$	2.2	0.42	9.1	57.0	NA	1.75	Au/Spiro-OMeTAD/ $CsSnBr_3$/TiO_2/SnO_2:F[b]	EQE, In-house	*Weizmann Institute of Science* [52]. Spin coating. The EQE integration gives 2 mA cm^{-2} less current density.
$CsSnI_3$	4.8	0.382	25.7	49.1	∼0.15	1.30	Au/PTAA/$CsSnI_3$/TiO_2/ SnO_2:F[b]	EQE, In-house	*Northwestern University and Mitsubishi Chemical Group Science & Technology Research Center* [53]. Spin coating with hydrazine. Integrated EQE gives J_{sc} of approximately 24 mA cm^{-2}.
$CsSn_{0.5}Ge_{0.5}I_3$	7.1	0.63	18.6	60.6	0.1	1.50	Au/Spiro-OMeTAD/ $CsSn_{0.5}Ge_{0.5}I_3$/PCBM/ SnO_2:F[b]	EQE, In-house	*Brown U., U. of Nebraska-Lincoln, Worcester Polytechnic Institute, and Okinawa Institute of Science and Technology Graduate University* [54]. Powder synthesized by solid-state reaction and thermally evaporated.

(Continued)

Table 2. (Continued.)

Material	Eff. (%)	V_{OC} (V)	J_{SC} (mA cm^{-2})	FF (%)	Area (cm^2)	E_g (eV)	Device structure	Means of verification	Institutions and Comments
Mixed-anions									
Q-1D Sb_2S_3-SbSI	6.08	0.62	14.92	0.66	0.16	1.76/2.1	Au/PCPDTBT/Sb_2S_3-SbSI/mp-TiO_2/TiO_2-BL/SnO_2:F[b]	EQE, in-house	*Ulsan National Institute of Science and Technology, Republic of Korea* [55]. Sb_2S_3 by chemical bath deposition and SbSI by hot plate of powders.
Q-1D SbSI	3.05	0.58	9.11	57.7	0.16	2.15	Au/PCPDTBT/SbSI/mp-TiO_2/TiO_2-BL/SnO_2:F[b]		*Ulsan National Institute of Science and Technology, Convergence Research Center for Solar Energy DGIST and Korea Research Institute of Chemical Technology (KRICT), Republic of Korea* [56]. Sb_2S_3 by chemical bath deposition, SbI_3 by spin coating and further soft hot plate. 10–20 cycles.
Q-1D $Sb_{0.67}Bi_{0.33}SI$	4.07	0.53	14.54	57.7	0.16	1.62	Au/PCPDTBT/$Sb_{0.67}Bi_{0.33}SI$/mp-TiO_2/TiO_2-BL/SnO_2:F[b]	EQE, in-house	*Ulsan National Institute of Science and Technology and Korea Research Institute of Chemical Technology (KRICT), Republic of Korea* [57]. Sb_2S_3 by chemical bath deposition, BiI_3 by spin coating and further soft hot plate, with repeated cycles.
Q-1D BiSI	1.32	0.445	8.44	35.14	0.04[a]	1.57	Au/F8/BiSI/SnO_2/SnO_2:F[b]	EQE, in-house	*U. Bristol* [58]. Spin coating and soft annealing.
Chalcogenides									
Se	6.5	0.969	10.6	63.4	0.027[a]	1.95	Glass/FTO/TiO_2/ZnMgO/Se/MoO_3/Au	EQE, In-house	*IBM Thomas J. Watson Research Centre, Yorktown Heights, USA* [59]. Thermal evaporation of Se at room temperature followed by post-deposition annealing.
GeSe	1.5	0.240	14.5	42.6	0.09[a]	1.1–1.2	Glass/ITO/CdS/GeSe/Au	EQE, In-house	*Beijing National Laboratory for Molecular Sciences, Key Laboratory of Molecular Nanostructure and Nanotechnology, Institute of Chemistry, Beijing, China* [60]. Rapid thermal sublimation.

(Continued)

Table 2. (Continued.)

Material	Eff. (%)	V_{OC} (V)	J_{SC} (mA cm^{-2})	FF (%)	Area (cm^2)	E_g (eV)	Device structure	Means of verification	Institutions and Comments
Q-1D Sb_2S_3	7.5	0.711	16.1	65.0	0.16	1.7	Glass/FTO/TiO_2/mp-TiO2/Sb_2S_3/PCPDTBT/PEDOT:PSS/Au[b]	EQE, In-house	*Division of Advanced Materials, Korea Institute of Chemical Technology, Daejeon, Republic of Korea* [61]. Chemical bath deposition followed by additional sulfurization.
Q-1D $Sb_2(S_xSe_{1-x})_3$	10.5	0.664	23.8	66.3	0.09	1.55	Glass/FTO/$Sb_2(S_xSe_{1-x})_3$/Au	EQE, in house	*Hefei National Laboratory for Physical Sciences at Microscale, CAS Key Laboratory of Materials for Energy Conversion, Department of Materials Science and Engineering, School of Chemistry and Materials Science, University of Science and Technology of China, Hefei* [62].
Bi_2S_3	3.3	0.700	10.7	45.0	0.18	1.2	Glass/ITO/P3HT:Bi_2S_3/MoO_x/Au[b]	EQE, In-house	*Department of Chemical and Biological Engineering, Princeton University, USA* [63]. Percolated Bi_2S_3 network with P3HT.
$Cu_2CdGeSe_4$	4.2	0.464	23.3	39.0	0.02[a]	1.27	Graphite/Epoxy/CCdGeSe/CdS/ZnO/AZO/glue/Ag/glass	EQE, In-house	*Tallinn University of Technology* [64]. Absorber prepared by molten salt method using CdI_2 and KI as fluxes. Monograin-based device.

[a] Area of the non certified cell below 0.1 cm^2 or not reported.

[b] Devices includes at least one organic carriers transport layer.

NA—not available; PC—phtalocyanine.

well-established solar cell technologies. However, for the emerging solar cell technologies that are developing very quickly, such certification is not always practical, so only in-house measured photovoltaic (PV) efficiencies are often reported. Thus, it is important to review here common best practices for in-house solar cell efficiency measurements. The most basic requirements for lab-based solar cell efficiency measurements include:

(a) using the air mass 1.5 spectrum (AM1.5) for terrestrial cells by choosing the highest-quality solar simulator available;
(b) applying one-sun of illumination with intensity of 1000 W cm^{-2} by adjusting the cell/simulator distance to match the expected current of the reference cell;
(c) controlling cell temperature during the measurement to 25 °C using active cooling or heating;
(d) using four-point probe geometry to remove the effect of probe/cell contact resistance.

In addition, there are several other best practices to follow.

(a) Areas of the measured solar cells have to be carefully defined using device isolation and/or light masking; this is particularly relevant to absorbers with large carrier diffusion lengths.
(b) Current density–voltage measurements have to be performed in both forward and reverse directions, which is especially important for emerging absorbers with tendency for hysteresis.
(c) EQE measurement has to be reported to assist with spectral correction, and integrated with the AM1.5 reference spectrum to obtain the current, to be compared to reported J_{sc}.
(d) Statistical analysis results, including the number of the solar cells measured, and the mean values have to be mentioned.
(e) Short-time evolution of the reported deficiency has to be verified at the maximum power point or with the photocurrent at maximum power point.
(f) Long-time stability analysis is encouraged, under light and electrical bias, with measured temperature and humidity.
(g) For multi-junction solar cells, the illumination bias and voltage bias used for each cell have to be reported.

Finally, we reemphasize that these are just guidelines for in-house solar cell measurements, when external certification is not practical. However, researchers working on emerging solar cell technologies are strongly encouraged to strive towards perfection and consider submission of their devices to one of the internationally recognized institutions.

2. Efficiency tables

Table 1 presents the list of materials that have been identified for the authors as certified solar cells, and are considered as the highest reported conversion efficiency in their class of technology. The last part of table 1 collects the technologies that being certified, do not fulfil some of the criteria used for including them in the principal section. Table 2 contains the list of materials and device performance for non-certified solar cells. The combined data from both tables is plotted in figure 2, where it is separated into three categories: metal pnictides (e.g. $ZnSnP_2$), chalcogenides (e.g. PbS), and halides (e.g. BiI_3).

3. New entries

3.1. Oxides

There have been no new records reported for solar cells with oxide absorbers, but several important advances have been made. For Cu_2O absorbers with Ga_2O_3 buffer layers grown by chemical vapour deposition, the V_{oc} of 1.78 V has been achieved albeit with small photocurrent of 2 mA cm^{-2} [65]. This demonstrates the ability of Cu_2O to reach >80% of V_{oc} entitlement based on Shockley–Queisser limit ($E_g = 2.2$ eV), and achieve in the future >13% efficiency for thicker absorber layers based on numerical models [66]. A low damage magnetron sputtering method for fabrication of ZnO contacts to Cu_2O solar cells has been also recently demonstrated [67]. The progress in Cu_2O and other oxide solar cells has been summarized in a recent roadmap article [67] and a book chapter [68].

As of the more exotic oxide absorbers with perovskite structure and ferroelectric properties, up to 4.2% efficiency has been reported in mixed-phase $BiMnO_3$ and $BiMn_2O_5$ thin film absorbers [18]. The reported V_{oc} of 1.5 V, J_{sc} of 7 mA cm^{-2} and fill factor of 0.58 have been reported (table 2). This report comes from the same group that published on 3.3% efficiency in single layers and 8.1% in multilayers of Bi_2FeCrO_6 6 years ago [41]. Neither of these exciting results published high profile journals have been replicated by other

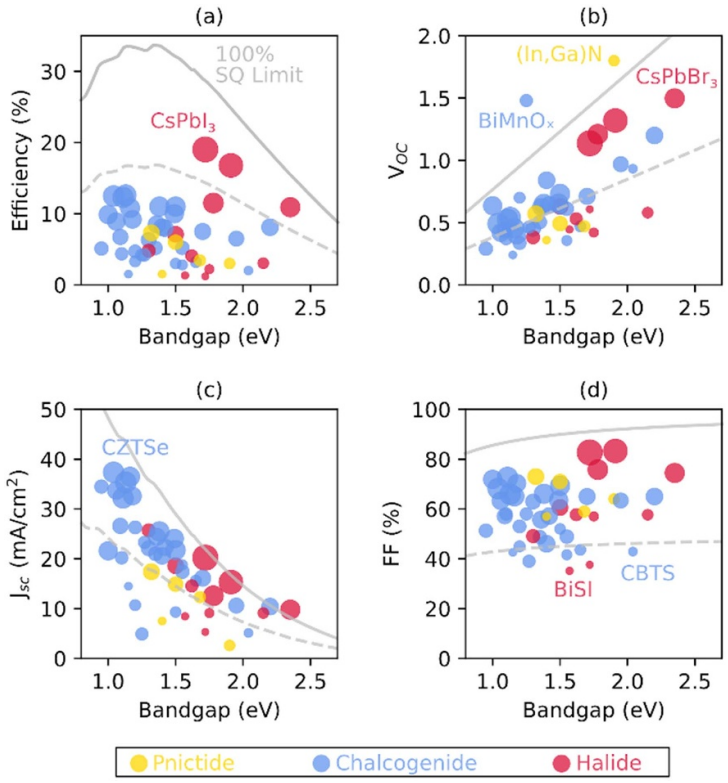

Figure 2. Efficiency (a), V_{oc} (b), J_{sc} (c) and FF (d) of the most relevant thin film inorganic PV technologies, from tables 1 and 2. Their performance is compared to the full Shockley–Queisser (SQ) limit for the AM1.5 spectrum (solid grey line) and 50% of the SQ limit (dashed grey line).

groups, which is somewhat concerning. The progress in $BiFeO_3$ derivatives [69] and other perovskites as photoferroic materials has been recently reviewed [70].

3.2. Chalcogenides

Five new results are reported in the present version for chalcogenides, with two new results from kesterite and antimony chalcogenide respectively, and three new entries from kesterite. The first new result is 12.5% efficiency pure selenide kesterite ($Cu_2ZnSnSe_4$) solar cell fabricated on glass shown in table 1. This highest efficiency pure selenide CZTSe solar cell also demonstrates the smallest V_{oc}-deficit (given by $E_g/q - V_{oc}$) of any reported kesterite family devices. The reported efficiency improvement is realized by engineering the local chemical environment (i.e. proper chemical composition and complete oxidation of Sn to Sn^{4+}) during the growth of kesterite thin-film, particularly at the point in time when the formation of kesterite initiates. With this defect control method, the reported electrical properties (i.e. mobility, carrier concentration) of kesterite are improved and the detrimental intrinsic defects are suppressed. One of three new entries for kesterite in table 2 is the magnesium-alloyed kesterite. The introduction of small amount of Mg into kesterite results in the 7.2% efficiency $Cu_2Zn_{0.96}Mg_{0.04}Sn(S,Se)_4$ solar cells. Such small amount Mg can lead to the change in lattice constant and carrier concentration of kesterite, which seems to play a similar role to alkaline Lithium. Notable substitution of group III elements of In and Ga in $Cu_2ZnSn(S,Se)_4$ were also reported to improve the efficiency even though the reasons for improvements are not thoroughly investigated [31]. Cd-substituted CZTS is recently reported with a new record of 12.6% [30] by engineering the charge extraction layers. We also note that a significant numbers of groups have reported efficiencies exceeding 12% [8, 30, 71] and closing the gap with world record efficiency reported by IBM in 2013 [6]. Most of these reports, however, have not completely eliminated the origin of the deep defects which are widely believed to cause band tailing and the significant V_{oc} deficit in this class of materials. Recent theoretical analysis and experimental evidence seem to indicate that a major contribution to the band tails is from the deep $2Cu_{Zn} + Sn_{Zn}$ defect clusters [72, 73]. The latest experimental evidence is demonstrated in the Cu_2CdZnS_4 (CCTS) where Cd substitution of Zn in Cu-poor CCTS suppress the deleterious $2Cu_{Zn} + Sn_{Zn}$ defect clusters and significantly reduces bandgap fluctuations [21]. This work sets a new efficiency record in Cu_2CdZnS_4 with 7.96%, which is the highest efficiency among the novel compounds derived from Cu–Zn–S/Se.

Another two new entries in table 2 are from simple chalcogenides, i.e. 5.1% efficiency Cu_2SnS_3 and 6.73% efficiency Ge-alloyed Cu_2SnS_3. Notable that Sn/Ge gradient is realized in the latter $Cu_2Sn_{1-x}Ge_xS_3$ (CTGS).

3.3. Pnictides

There have been several recent reports on $ZnSnP_2$ based solar cells [74]. The highest 3.4% efficiency reported to date is for $ZnSnP_2$ single crystal absorbers with (Cd, Zn)S buffer layers [17], with J_{sc} of 12 mA cm^{-2}, V_{oc} of 0.47 and a fill factor of 0.59 (table 2). Thin film $ZnSnP_2$ solar cell with CdS buffer layers prepared by phosphidation of Zn/Sn stacks had much lower efficiencies (0.02%) [75] compared to crystal based ZnSnP2/CdS solar cells (2%) [76]. All-phosphide $ZnSnP_2$ single crystal devices with $CdSnP_2$ buffer layers showed clear rectification behaviour but no photoresponse [77].

3.4. Halides

The number of published papers reporting halide materials for PV (mainly perovskite halides), are increasing quickly, and in consequence several progresses have been reported. Most of the high efficiency absorbers becomes from the Cs–Pb perovskite halide family, and have shown 1%–3% record efficiency improvement in the last year. Some of these progresses are related to the use of additives for the best control of growth procedure and crystallization process.

$CsPbI_3$—the record efficiency has improved up to an impressive 19.03%. Wang *et al* [47] demonstrated that the use of DMAI is very effective to manipulate the crystallization process of $CsPbI_3$, confirming that the DMAI additive would not alloy into the crystal lattice of $CsPbI_3$ perovskite. Furthermore, the use of phenyltrimethylammonium chloride passivated $CsPbI_3$ inorganic perovskite, allowing for the impressive efficiency improvement, although there is a debate if DMA and DMAI can sit at the A-sites of the perovskite structure and these materials are non-fully inorganic.

$CsPbBr_3$—although more modest, $CsPbBr_3$ has achieved a new record of 10.91%. To do so, Tong *et al* [46] developed a growth procedure induced by phase transition that makes the grain size of perovskite films more uniform, and also lowers the surface potential barrier that exists between the crystals and grain boundaries.

$CsPbBrI_2$ and $CsPbIBr_2$—in the first case only limited efficiency improvement has been reported in the last months, achieving 16.79% efficiency record with and impressive V_{oc} of 1.32 V. This improvement was again related to passivation effect and n-type doping by introducing $CaCl_2$, observing also that the crystallinity of the $CsPbI_2Br$ perovskite film was enhanced, and the trap density was suppressed through the use of $CaCl_2$ treatment [48]. In the second case, a record efficiency of 11.10% has been reported with an improved V_{oc} of 1.21 V, but with a large enhancement of the FF up to 74.82% [49]. This has been possible thanks to the introduction of a Lewis base (PEG) as additive observing suppressed non-radiative electron–hole recombination and a favourable energy band structure.

Other halide perovskites do not report important progresses in terms of conversion efficiency in the last months.

3.5. Mixed-anion

Starting from this second edition of the efficiency tables, we are including a new class of PV absorbers based on mixed antimony and/or bismuth chalcogenide-halides. Special mention merits the work of Neo and Seok [55], where using a fast vapour process they developed SbSI and SbSI-interlayered Sb_2S_3 solar cells, demonstrating a TiO_2/Sb_2S_3/SbSI/HTM device with a conversion efficiency of 6.08%. Efficiencies between 1% and 4% have been also reported for SbSI, (Sb, Bi)SI and BiSI systems, demonstrating the large potential of these mixed chalcogenide-halide compounds and the increased interest that the scientific community is putting in such materials for solar cells applications.

4. Latest progresses in selected topic: Q-1D absorbers for PV

Traditionally, absorber materials for PVs are limited to semiconductors with three-dimensional (3D) crystal structure (i.e. GaAs, CdTe and Cu(In, Ga)Se_2) thus enjoying the nearly isotropic film growth and carrier transport. Recently, the previously abandoned low-dimensional absorber materials have attracted wide attention because of their simple and Earth-abundant composition, and performance improvement [4, 60, 78]. Specifically, the Q-1D binary antimony-based chalcogenide (Sb_2S_3, Sb_2Se_3 and $Sb_2(S,Se)_3$ alloy) solar cells are nontoxic and stable, and have achieved impressive power conversion efficiency of 7%–10% [4, 12, 79]. Q-1D Sb-based chalcogenides are made up of covalently bonded $[Sb_4S(e)_6]_n$ ribbons, and these ribbons are stacked via weak Van der Waals force along *a*- and *b*-axis [80]. Based on device configuration, Q-1D Sb-based chalcogenide solar cells can be divided into sensitized solar cells and planar (superstrate and

substrate) devices. Next, we will briefly review the main efficiency improvement of Q-1D solar cells in each configuration:

Sensitized-type solar cell. At the early age, Sb-based chalcogenide sensitized-type solar cells was led by Seok group from Korea Research Institute of Chemical Technology. The typical device configuration is TCO/bl-TiO_2/mp-TiO_2/$Sb_2S(e)_3$/HTL/metal (here, TCO = transparent conducting oxide; bl = block layer; mp = mesoporous; HTL = hole transport layer). The current champion efficiency of Sb_2S_3, Sb_2Se_3 and $Sb_2(S, Se)_3$ sensitized-type solar cells were achieved in 2014 as 7.5% [61], 3.21% [81] and 6.6% [82], respectively. The absorber layers were exclusively based on the solution processing, and the device configuration is relatively complex. No significant progress for sensitized solar cells has been reported since 2014.

Superstrate solar cells. For superstrate Sb_2S_3 solar cells, the first >5% efficiency was reported in 2014 through atomic layer deposition (ALD) [83]. Chen's group from University of Science and Technology of China obtained 6.35% efficiency using hydrothermally processed Sb_2S_3 at 2018 [84]; they further improved device efficiency to 6.5% via Cs-doped Sb_2S_3 at 2019 [85]. For Sb_2Se_3 solar cells, Tang's group from Huazhong University of Science and Technology led the progresses: they reported the first planar-type Sb_2Se_3 solar cells at 2014 using hydrazine solution processing [86]; they introduced rapid thermal evaporation to obtain high-quality Sb_2Se_3 film and achieved a certified efficiency of 5.6% at 2015 [87]; they further employed vapour transfer deposition (VTD) to fabricate Sb_2Se_3 films and obtained a certified efficiency of 7.6% [12]. Very recently, Liang *et al* and Cheng at al. suppressed the deep defects (V_{Se} and Sb_{Se}) in Sb_2Se_3 by the means of postselenization or *in situ* selenium compensation. Consequently, a large V_{OC} of ~0.5 V was obtained; however, the efficiency was lower than 7% because of the inferior J_{SC} [88–90]. For $Sb_2(S,Se)_3$ solar cells, Tang's group used the VTD technique to fabricate $Sb_2(S, Se)_3$ solar cells and obtained a champion efficiency of 6.3% in 2019 [91]. Subsequently, Chen's group adopted the hydrothermal method to fabricate $Sb_2(S, Se)_3$ solar cells, which lead to absorber film with less defects, and obtained a device efficiency of 7.82% [79]. They further optimized the device to a certified efficiency of 10.0%, the current efficiency record for all Q1-D Sb-chalcogenide solar cells. Device stability subjected to damp-heat, light-soaking, ultraviolet ageing and thermal cycling testing is also satisfactory, nearly fully surpassing the IEC61646 standard for a ZnO/Sb_2Se_3 superstrate device [78].

Substrate solar cells. Research on substrate Sb-based chalcogenide solar cells lags behind superstrate devices possibly because of their more complex configuration and time-consuming fabrication. Until now, the champion efficiency of Sb_2S_3 substrate solar cell is only 1.75% [92]; and no substrate $Sb_2(S, Se)_3$ solar cells is reported in literatures. Tang's group reported the first substrate Sb_2Se_3 solar cells in 2014 [93]. Then Mai's group from Hebei University made significant progress in this field and they successfully obtained a certified record efficiency of 9.2% in 2019 employing the close spaced sublimation to fabricate Sb_2Se_3 absorber [4].

The Q-1D crystal structure of Sb-based chalcogenides result in some unique features as compared with conventional 3D PV materials. Film orientation along the $[Sb_4S(e)_6]_n$ ribbon direction is highly preferred for high efficiency devices; otherwise photogenerated carriers have to hop between these ribbons leading to high series resistance and low J_{sc} and FF. One additional benefit of proper orientation is benign grain boundaries because of no dangling bond at the side of ribbons, and these advantages offer an opportunity for flexible device [87]. Orientation engineering is thus intensively investigated: fast deposition to induce kinetic controlled growth [94], carefully optimized substrate to enable strong bonding at the interface via (quasi) epitaxy or reaction [95], and a pre-screening seed strategy [96], have proved to be effective in obtaining preferred (hkl) $l \neq 0$ orientation.

There are a few challenges to be solved for further efficiency improvement, particularly the low V_{oc}: (a) effective p-type doping to obtain ~10^{16} cm^{-3} doping density remains elusive; large atoms such as Pb and Sn could be promising to induce substitutional p-type doping instead of interstitial n-type doping into the gap between ribbons. (b) Complicated deep defects have recently been predicted by first-principle calculation because of the non-equivalent Sb and S/Se sites and spacious volume in Sb-based chalcogenides [97]. Confirming and subsequent removal of these defects are required for V_{oc} and efficiency improvement. (c) Spectroscopic results indicated that strong self-trapped exciton exist in Sb-based chalcogenides due to the soft lattice and strong exciton–phonon coupling [98, 99], resulting in fundamental energy loss. Whether this is true and universal for Q1-D Sb-based chalcogenides calls for further verification. (d) The carrier lifetime is generally short for Sb-based chalcogenide solar cells [98, 99]; passivation of deep defects in the bulk and at the surface (or interface) requires further efforts.

Overall, the unique crystal structure and the rapid efficiency progress make Q-1D Sb-based chalcogenides scientifically interesting and technologically promising. A further efficiency improvement, combined with the proven features of outstanding flexibility, light weight, high stability, non-toxicity and low cost, promises Q-1D Sb-based chalcogenide solar cells a bright future as the energy supplier for internet of things sensors.

Acknowledgments

E S thanks H2020 EU Programme under the projects SENSATE (H2020-ERC-CoG-2019-866018) and CUSTOM-ART (H2020-LC-SC3-2020-RES-IA-CSA-952982), and the Spanish Ministry of Science, Innovation and Universities for the IGNITE Project (ENE2017-87671-C3-1-R). L H W thanks Shreyash Hadke for compiling the selected literature for complex chalcogenides and acknowledges funding from CREATE Programme under the Campus for Research Excellence and Technological Enterprise (CREATE), which is supported by the National Research Foundation, Prime Minister's Office, Singapore; and Ministry of Education (MOE) Tier 2 Project (MOE2016-T2-1-030). A Z was supported by the U.S. Department of Energy (DOE) under Contract No. DEAC36-08GO28308 with the Alliance for Sustainable Energy, LLC, the manager and operator of the National Renewable Energy Laboratory (NREL). A Z would like to thank Nikos Kopidakis at NREL for useful discussions. The views expressed in the article do not necessarily represent the views of the DOE or the U.S. Government. X H acknowledges funding support from Australian Renewable Energy Agency (ARENA, 1-USO028 and 2017/RND006) and Australian Research Council (ARC) (future fellowship programme, FT190100756). J T acknowledge the financial support by the National Natural Science Foundation of China (61725401) and the Major State Basic Research Development Program of China (2016YFA0204000).

Authors description and contribution

Dr Andriy Zakutayev, National Renewable Energy Laboratory, Golden, CO 80401, United States of America (e-mail: andriy.zakutayev@nrel.gov): contributed to compile the information about oxides and pnictides, and to write sections 1.4, 3.1 and 3.3.

Prof. Jonathan D Major, Stephenson Institute for Renewable Energy, Department of Physics, University of Liverpool, Liverpool L69 7ZF, United Kingdom (e-mail: jon.major@liverpool.acuk): contributed to compile the information about simple chalcogenides (three atoms or less), and to write section 3.2.

Prof. Xiaojing Hao, Australian Centre for Advanced Photovoltaics, School of Photovoltaic and Renewable Energy Engineering, University of New South Wales, Sydney, NSW 2052, Australia (e-mail: xj.hao@unsw.edu.au): contributed to compile the information about complex chalcogenides (three atoms or more), and to write section 3.2.

Prof. Aron Walsh, Department of Materials, Imperial College London, Exhibition Road, London SW7 2AZ, United Kingdom; and Yonsei University, South Korea (e-mail: a.walsh@imperial.acuk): contributed to compile all the information in graphic format in section 2.

Prof. Jiang Tang, Wuhan National Laboratory for Optoelectronics, Huazhong University of Science and Technology, 430074 Wuhan, People's Republic of China (e-mail: jtang@hust.edu.c): contributed to write the section 4.

Dr Teodor K Todorov, IBM Thomas J Watson Research Center, Yorktown Heights, New York 10598, United States of America (e-mail: tktodoro@us.ibm.com): contributed to compile the information about simple chalcogenides (three atoms or less), and to write section 3.2.

Prof. Lydia H Wong, School of Materials Science & Engineering, Nanyang Technological University, 639798, Singapore (e-mail: lydiawong@ntu.edu.sg): contributed to compile the information about complex chalcogenides (four atoms or more), and to write section 3.2.

Prof. Edgardo Saucedo, Universitat Politècnica de Catalunya (UPC), Campus Diagonal-Besòs, 08930 Sant Adrià del Besòs- Barcelona, Spain (e-mail: edgardo.saucedo@upc.edu): act as leader and corresponding author of the paper. Contributed to compile the information about halides and mixed chalcogenide-halides, and build the complete version of the efficiency tables, and to write sections 1.1–1.3, and 3.4.

All the authors contributed equally to define the structure and content of the manuscript, to the general review and final approval of the paper.

Disclaimer

The information in this paper was selected in good faith by all the authors. Errors and omissions will be corrected in the subsequent editions of the table. Corrections and more complete information from the scientific community is most welcome in order to improve the accuracy of the values presented in the efficiency tables.

Please note that due to being an update of 'Emerging inorganic solar cell efficiency tables (version 1)' by these authors, it was agreed with IOP Publishing that this manuscript needs to contain text replicated from the earlier version to ensure consistency of format and enable the current paper to be read as a standalone document. This is an exception to the policy of the journal on text recycling.

ORCID iDs

Andriy Zakutayev https://orcid.org/0000-0002-3054-5525
Aron Walsh https://orcid.org/0000-0001-5460-7033
Lydia H Wong https://orcid.org/0000-0001-9059-1745
Edgardo Saucedo https://orcid.org/0000-0003-2123-6162

References

[1] Green M A, Dunlop E D, Hohl-Ebinger J, Yoshita M, Kopidakis N and Hao X 2020 *Prog. Photovolt., Res. Appl.* **28** 629
[2] Almora O *et al* 2020 *Adv. Energy Mater.* 2002774
[3] Wong L H, Zakutayev A, Major J D, Hao X, Walsh A, Todorov T K and Saucedo E 2019 *J. Phys. Energy* **1** 032001
[4] Li Z *et al* 2019 *Nat. Commun.* **10** 125
[5] Yan C *et al* 2018 *Nat. Energy* **3** 764
[6] Wang W, Winkler M T, Gunawan O, Gokmen T, Todorov T K, Zhu Y and Mitzi D B 2014 *Adv. Energy Mater.* **4** 1301465
[7] Son D-H *et al* 2019 *J. Mater. Chem.* A **7** 25279
[8] Li J *et al* 2020 *Adv. Mater.* **32** 2005268
[9] Lee Y S, Chua D, Brandt R E, Siah S C, Li J V, Mailoa J P, Lee S W, Gordon R G and Buonassisi T 2014 *Adv. Mater.* **26** 4704
[10] Sanehira E M, Marshall A R, Christians J A, Harvey S P, Ciesielski P N, Wheeler L M, Schulz P, Lin L Y, Beard M C and Luther J M 2017 *Sci. Adv.* **3** eaao4204
[11] Sinsermsuksakul P, Sun L, Lee S W, Park H H, Kim S B, Yang C and Gordon R G 2014 *Adv. Energy Mater.* **4** 1400496
[12] Wen X *et al* 2018 *Nat. Commun.* **9** 2179
[13] Tang R *et al* 2020 *Nat. Energy* **5** 587
[14] Yang X *et al* 2017 *Nano-Micro Lett.* **9** 24
[15] Bernechea M, Miller N C, Xercavins G, So D, Stavrinadis A and Konstantatos G 2016 *Nat. Photon.* **10** 521
[16] Bhushan M and Catalano A 1981 *Appl. Phys. Lett.* **38** 39
[17] Akari S, Chantana J, Nakatsuka S, Nose Y and Minemoto T 2018 *Sol. Energy Mater. Sol. Cells* **174** 412
[18] Chakrabartty J, Harnagea C, Celikin M, Rosei F and Nechache R 2018 *Nat. Photon.* **12** 271
[19] Welch A W, Baranowski L L, Peng H, Hempel H, Eichberger R, Unold T, Lany S, Wolden C and Zakutayev A 2017 *Adv. Energy Mater.* **7** 1601935
[20] Banu S, Ahn S J, Ahn S K, Yoon K and Cho A 2016 *Sol. Energy Mater. Sol. Cells* **151** 14
[21] Hadke S, Levcenko S, Sai Gautam G, Hages C J, Márquez J A, Izquierdo-Roca V, Carter E A, Unold T and Wong L H 2019 *Adv. Energy Mater.* **9** 1902509
[22] Chen Z, Sun K, Su Z, Liu F, Tang D, Xiao H, Shi L, Jiang L, Hao X and Lai Y 2018 *ACS Appl. Energy Mater.* **1** 3420
[23] Ge J, Koirala P, Grice C R, Roland P J, Yu Y, Tan X, Ellingson R J, Collins R W and Yan Y 2017 *Adv. Energy Mater.* **7** 1601803
[24] Chatterjee S and Pal A J 2017 *Sol. Energy Mater. Sol. Cells* **160** 233
[25] Zhao W, Wang G, Tian Q, Huang L, Gao S and Pan D 2015 *Sol. Energy Mater. Sol. Cells* **133** 15
[26] Shin D, Zhu T, Huang X, Gunawan O, Blum V and Mitzi D B 2017 *Adv. Mater.* **29** 1606945
[27] Schnabel T, Seboui M, Bauer A, Choubrac L, Arzel L, Harel S, Barreau N and Ahlswede E 2017 *RSC Adv.* **7** 40105
[28] Choubrac L *et al* 2020 *ACS Appl. Energy Mater.* **3** 5830
[29] Gershon T, Sardashti K, Gunawan O, Mankad R, Singh S, Lee Y S, Ott J A, Kummel A and Haight R 2016 *Adv. Energy Mater.* **6** 1601182
[30] Su Z *et al* 2020 *Adv. Mater.* **32** 2000121
[31] Qi Y-F, Kou D-X, Zhou W-H, Zhou Z-J, Tian Q-W, Meng Y-N, Liu X-S, Du Z-L and Wu S-X 2017 *Energy Environ. Sci.* **10** 2401
[32] Hadke S H, Levcenko S, Lie S, Hages C J, Márquez J A, Unold T and Wong L H 2018 *Adv. Energy Mater.* **8** 1802540
[33] Kim S, Kim K M, Tampo H, Shibata H and Niki S 2016 *Appl. Phys. Express* **9** 102301
[34] Cabas-Vidani A *et al* 2018 *Adv. Energy Mater.* **8** 1801191
[35] Li X, Hou Z, Gao S, Zeng Y, Ao J, Zhou Z, Da B, Liu W, Sun Y and Zhang Y 2018 *Sol. RRL* **2** 1800198
[36] Caballero R, Haass S G, Andres C, Arques L, Oliva F, Izquierdo-Roca V and Romanyuk Y E 2018 *Front. Chem.* **6** 1
[37] Chantana J, Tai K, Hayashi H, Nishimura T, Kawano Y and Minemoto T 2020 *Sol. Energy Mater. Sol. Cells* **206** 110261
[38] Yu X, Cheng S, Yan Q, Fu J, Jia H, Sun Q, Yang Z and Wu S 2020 *Sol. Energy Mater. Sol. Cells* **209** 110434
[39] Umehara M, Tajima S, Aoki Y, Takeda Y and Motohiro T 2016 *Appl. Phys. Express* **9** 072301
[40] Minami T, Nishi Y and Miyata T 2013 *Appl. Phys. Express* **6** 044101
[41] Nechache R, Harnagea C, Li S, Cardenas L, Huang W, Chakrabartty J and Rosei F 2015 *Nat. Photon.* **9** 61
[42] Nian Q, Montgomery K H, Zhao X, Jackson T, Woodall J M and Cheng G J 2015 *Appl. Phys.* A **121** 1219
[43] Dahal R, Li J, Aryal K, Lin J Y and Jiang H X 2010 *Appl. Phys. Lett.* **97** 073115
[44] Javaid K, Wu W, Wang J, Fang J, Zhang H, Gao J, Zhuge F, Liang L and Cao H 2018 *ACS Photonics* **5** 2094
[45] Tiwari D, Alibhai D and Fermin D J 2018 *ACS Energy Lett.* **3** 1882
[46] Tong G, Chen T, Li H, Qiu L, Liu Z, Dang Y, Song W, Ono L K, Jiang Y and Qi Y 2019 *Nano Energy* **65** 104015
[47] Wang Y, Liu X, Zhang T, Wang X, Kan M, Shi J and Zhao Y 2019 *Angew. Chem., Int. Ed.* **58** 16691
[48] Han Y, Zhao H, Duan C, Yang S, Yang Z, Liu Z and Liu S F 2020 *Adv. Funct. Mater.* **30** 1909972
[49] You Y, Tian W, Wang M, Cao F, Sun H and Li L 2020 *Adv. Mater. Interfaces* **7** 2000537
[50] Li N, Zhu Z, Li J, Jen A K Y and Wang L 2018 *Adv. Energy Mater.* **8** 1800525
[51] Akin S *et al* 2018 *Joule* **3** 205
[52] Gupta S, Bendikov T, Hodes G and Cahen D 2016 *ACS Energy Lett.* **1** 1028
[53] Bin Song T, Yokoyama T, Aramaki S and Kanatzidis M G 2017 *ACS Energy Lett.* **2** 897
[54] Chen T *et al* 2018 *Nat. Commun.* **10** 16
[55] Nie R and Seok S I 2020 *Small Methods* **4** 1900698
[56] Nie R, Yun H, Paik M-J, Mehta A, Park B, Choi Y C and Seok S I 2018 *Adv. Energy Mater.* **8** 1701901
[57] Nie R, Im J and Seok S I 2019 *Adv. Mater.* **31** 1808344
[58] Tiwari D, Cardoso-Delgado F, Alibhai D, Mombrú M and Fermín D J 2019 *ACS Appl. Energy Mater.* **2** 3878

[59] Todorov T K, Singh S, Bishop D M, Gunawan O, Lee Y S, Gershon T S, Brew K W, Antunez P D and Haight R 2017 *Nat. Commun.* **8** 682
[60] Xue D-J, Liu S-C, Dai C-M, Chen S, He C, Zhao L, Hu J-S and Wan L-J 2017 *J. Am. Chem. Soc.* **139** 958
[61] Choi Y C, Lee D U, Noh J H, Kim E K and Seok S I 2014 *Adv. Funct. Mater.* **24** 3587
[62] Wang X, Tang R, Jiang C, Lian W, Ju H, Jiang G, Li Z, Zhu C and Chen T 2020 *Adv. Energy Mater.* **2** 2002341
[63] Whittaker-Brooks L, Gao J, Hailey A K, Thomas C R, Yao N and Loo Y-L 2015 *J. Mater. Chem.* C **3** 2686
[64] Kauk-Kuusik M *et al* 2018 *Thin Solid Films* **666** 15
[65] Chua D, Kim S B and Gordon R 2019 *AIP Adv.* **9** 055203
[66] Miyata T, Watanabe K, Tokunaga H and Minami T 2019 *J. Semicond.* **40** 032701
[67] Coll M *et al* 2019 *Appl. Surf. Sci.* **482** 1
[68] Pérez-Tomás A, Mingorance A, Tanenbaum D and Lira-Cantú M 2018 *Futur. Semiconductor Oxides Next-Generation Solor Cells* (Amsterdam: Elsevier) pp 267–356
[69] Chen G, Chen J, Pei W, Lu Y, Zhang Q, Zhang Q and He Y 2019 *Mater. Res. Bull.* **110** 39
[70] Bai Y, Jantunen H and Juuti J 2019 *ChemSusChem* **12** 2540
[71] Green M A, Hishikawa Y, Dunlop E D, Levi D H, Hohl-Ebinger J, Yoshita M and Ho-Baillie A W Y 2019 *Prog. Photovolt., Res. Appl.* **27** 3
[72] Rey G, Larramona G, Bourdais S, Choné C, Delatouche B, Jacob A, Dennler G and Siebentritt S 2018 *Sol. Energy Mater. Sol. Cells* **179** 142
[73] Crovetto A, Kim S, Fischer M, Stenger N, Walsh A, Chorkendorff I and Vesborg P C K 2020 *Energy Environ. Sci.* **13** 3489
[74] Nakatsuka S, Yuzawa N, Chantana J, Minemoto T and Nose Y 2017 *Phys. Status Solidi* **214** 1600650
[75] Yuzawa N, Chantana J, Nakatsuka S, Nose Y and Minemoto T 2017 *Curr. Appl. Phys.* **17** 557
[76] Nakatsuka S, Akari S, Chantana J, Minemoto T and Nose Y 2017 *ACS Appl. Mater. Interfaces* **9** 33827
[77] Nakatsuka S, Kazumi K and Nose Y 2019 *Japan. J. Appl. Phys.* **58** 075508
[78] Wang L *et al* 2017 *Nat. Energy* **2** 17046
[79] Jiang C *et al* 2020 *Cell Rep. Phys. Sci.* **1** 100001
[80] Chen C *et al* 2017 *Front. Optoelectron.* **10** 18
[81] Choi Y C, Mandal T N, Yang W S, Lee Y H, Im S H, Noh J H and Seok S I 2014 *Angew. Chem.* **126** 1353
[82] Choi Y C, Lee Y H, Im S H, Noh J H, Mandal T N, Yang W S and Seok S I 2014 *Adv. Energy Mater.* **4** 1301680
[83] Kim D, Lee S, Park M S, Kang J, Heo J H, Im S H and Sung S 2014 *Nanoscale* **6** 14549
[84] Tang R, Wang X, Jiang C, Li S, Liu W, Ju H, Yang S, Zhu C and Chen T 2018 *ACS Appl. Mater. Interfaces* **10** 30314
[85] Jiang C, Tang R, Wang X, Ju H, Chen G and Chen T 2019 *Sol. RRL* **3** 1800272
[86] Zhou Y *et al* 2014 *Adv. Energy Mater.* **4** 1301846
[87] Zhou Y *et al* 2015 *Nat. Photon.* **9** 409
[88] Liu X, Qiao Y, Liu Y, Liu J, Jia E, Chang S, Shen X, Li S and Cheng K 2020 *Sol. Energy* **195** 697
[89] Liang G-X *et al* 2020 *Nano Energy* **76** 105105
[90] Tang R, Zheng Z-H, Su Z-H, Li X-J, Wei Y-D, Zhang X-H, Fu Y-Q, Luo J-T, Fan P and Liang G-X 2019 *Nano Energy* **64** 103929
[91] Lu S, Zhao Y, Wen X, Xue D, Chen C, Li K, Kondrotas R, Wang C and Tang J 2019 *Sol. RRL* **3** 1800280
[92] Pan G, Wang D, Gao S, Gao P, Sun Q, Liu X, Zhou Z, Sun Y and Zhang Y 2019 *Sol. Energy* **182** 64
[93] Liu X *et al* 2014 *ACS Appl. Mater. Interfaces* **6** 10687
[94] Kondrotas R, Zhang J, Wang C and Tang J 2019 *Sol. Energy Mater. Sol. Cells* **199** 16
[95] Deng H *et al* 2019 *Adv. Funct. Mater.* **29** 1901720
[96] Li K, Chen C, Lu S, Wang C, Wang S, Lu Y and Tang J 2019 *Adv. Mater.* **31** 1903914
[97] Huang M, Xu P, Han D, Tang J and Chen S 2019 *ACS Appl. Mater. Interfaces* **11** 15564
[98] Yang Z *et al* 2019 *Nat. Commun.* **10** 4540
[99] Wang K, Chen C, Liao H, Wang S, Tang J, Beard M C and Yang Y 2019 *J. Phys. Chem. Lett.* **10** 4881